Altered pre-symptomatic AMPA and cannabinoid receptor trafficking in motor neurons of ALS model mice: implications for excitotoxicity

Pingwei Zhao, **Sheila Ignacio**, **Eric Beattie**[*], and **Mary E. Abood**[*]

Forbes Norris ALS/MDA Research Center. California Pacific Medical Center Research Institute. 475 Brannan St. Suite 220, San Francisco, CA 94107, USA

Abstract

Amyotrophic lateral sclerosis (ALS) is a fatal neurodegenerative disorder involving the selective loss of spinal cord motor neurons. Excitotoxicity mediated by glutamate has been implicated as a cause of this progressive degeneration. In this study we examined two types of receptors, the excitatory AMPA-type glutamate receptors (AMPARs) and inhibitory cannabinoid receptor (CB1) with respect to their localization and total expression in spinal cord motor neurons. AMPAR and CB1 represent major excitatory and inhibitory transmission input respectively and their expression levels on the plasma membrane have direct relevance to the vulnerability of the motor neurons to glutamatergic excitotoxicity. We used quantitative immunofluorescence microscopy to comparatively measure the total cellular expression and the synaptic localization of specific subclasses of AMPARs (as determined by the presence of the subunits GluR1 or GluR2) and cannabinoid receptors (CB1) in spinal cord motor neurons during disease progression in a G93ASOD1 mouse model of ALS. We found an increase in synaptic GluR1 and a decrease of synaptic and total GluR2 at early ages (6 weeks, prior to disease onset). Total CB1 receptor levels were decreased at 6 weeks of age. We determined gene expression of CB1, GluR1, and GluR2 using quantitative real time RT-PCR. The decreased synaptic and total GluR2 and increased synaptic GluR1 levels may result in increased numbers of Ca^{2+}-permeable AMPARs, thus contributing to neuronal death. Early alterations in CB1 expression may also predispose motor neurons to excitotoxicity. To our knowledge, this is the first demonstration of presymptomatic changes in trafficking of receptors that are in direct control of excitotoxicity and death in a mouse model of ALS.

Keywords

amyotrophic lateral sclerosis; AMPA receptor; cannabinoid receptor; excitotoxicity; G93A; glutamate receptor; spinal cord

Address correspondence to: Eric Beattie, CPMCRI, 475 Brannan St, Suite 220, San Francisco, CA 94107, USA, 415 600-1185 (office); 415 600-1174 (Fax); beattie@cpmcri.org, Mary E. Abood, CPMCRI, 475 Brannan St, Suite 220, San Francisco, CA 94107, USA, 415 600-3607 (office); 415 600-1725 (Fax); aboodm@cpmcri.org.
[*]These authors contributed equally to this work

Introduction

Amyotrophic lateral sclerosis (ALS) occurs at a rate of 1 in 50,000 and is the most lethal neurodegenerative disease (Boillee *et al.*, 2006). ALS results in the degeneration of motor neurons in the cortex, brainstem and spinal cord likely through a variety of etiologies (Brown, 1997; Boillee *et al.*, 2006). Most of the causes of ALS are presently unknown, however several mechanisms of insult to motor neurons have been suggested (Ludolph *et al.*, 2000; Robberecht, 2000; Cleveland & Rothstein, 2001). Two of the primary theories underlying motor neuron vulnerability are susceptibility to excitotoxicity and oxidative damage, including neuroinflammation (Ludolph *et al.*, 2000; Robberecht, 2000). Two classes of receptors in particular have been shown to feed directly into this process of excitotoxicity; the excitatory AMPA-type glutamate receptors (AMPARs) (Corona & Tapia, 2007) and the inhibitory cannabinoid CB1 receptor (CB1) (Abood *et al.*, 2001; Kim *et al.*, 2006b).

The AMPA receptors (α-amino-3-hydroxy-5-methyl-4-isoxazolepropionic acid receptors, AMPARs) play a central regulatory role in glutamate excitotoxicity in motor neurons (Carriedo *et al.*, 1996). AMPARs are tetrameric assemblies of subunits GluR1-4, and GluR1 homomeric AMPARs (AMPARs lacking the GluR2 subunit), or those containing unedited GluR2 (where Q is not replaced by R) have larger current carrying capacity and are calcium permeable (Pellegrini-Giampietro *et al.*, 1997). GluR1 homomeric AMPARs represent a class of these calcium permeable receptors increasingly seen in CNS disease and injury conditions (Leonoudakis *et al.*, 2004; Ogoshi *et al.*, 2005; Stellwagen *et al.*, 2005; Corona & Tapia, 2007). Any increase in the synaptic or surface localization or any change in the channel properties of AMPARs changes the excitatory profile of a neuron to a given amount of glutamate. Motor neurons contain a higher percentage of calcium permeable AMPARs, which could provide an explanation for their particular vulnerability to any putative excitotoxic stress throughout the progression of ALS (Carriedo *et al.*, 1996; Roy *et al.*, 1998; Bar-Peled *et al.*, 1999; Vandenberghe *et al.*, 2000).

The endocannabinoid system consists of the CB1 and CB2 G-protein coupled cannabinoid receptors, their endogenous lipid ligands (endocannabinoids) and the enzymes that synthesize and degrade the endocannabinoids. Recent studies have described the involvement of the endocannabinoid system in the progression of disease in hSOD1G93A mice and the benefits associated with the administration of cannabinoid agonists (Bilsland *et al.*, 2004; Raman *et al.*, 2004; Witting *et al.*, 2004; Weydt *et al.*, 2005; Kim *et al.*, 2006a; Shoemaker *et al.*, 2006). These results suggest that cannabinoid receptor-mediated processes may modify disease progression in amyotrophic lateral sclerosis and other chronic neurodegenerative diseases.

Mutations in Cu/Zn superoxide dismutase (hSOD1) are the primary cause of up to 20% of familial ALS cases (Rosen *et al.*, 1993). The hSOD1G93A mice is the strain predominantly used for preclinical testing of compounds for treating ALS; the disease in these animals follows a consistent onset, progression and outcome that closely mimics human ALS (Gurney *et al.*, 1996; Klivenyi *et al.*, 1999; Zhu *et al.*, 2002).

In this report, we have examined the total expression and synaptic localization of CB1 cannabinoid receptors and AMPARs in hSOD1G93A mouse spinal cord during disease progression using quantitative immunofluorescence microscopy. Additionally, we determined the gene expression of GluR1, GluR2, and CB1 using quantitative real time RT-PCR. The synaptic localization of these particular receptors has not previously been examined in the progression of an ALS animal model, yet this determination is relevant to disease progression since an increase in cannabinoid receptors may provide for protection against excitotoxicity while an increase in synaptic AMPARs may increase motor neuron susceptibility to excitotoxicity, especially as we found they are both expressed in motor neurons. Synaptic GluR1 levels are increased and synaptic and total GluR2 levels are decreased in spinal cord motor neurons as early as 6 weeks of age in the G93A mouse model of ALS.

Materials and Methods

Transgenic mice

Experiments were performed in accordance with the "NIH Guide for the Care and Use of Laboratory Animals" (NIH publication no. 86-23) and the guidelines approved by the California Pacific Medical Center animal care committee. Male transgenic mice expressing the human mutant SOD1G93A (B6SJL-TgN[SOD1-G93A]1Gur) (hSOD1G93A mice) or the wild type SOD1 (B6.Cg-Tg(SOD1)2Gur/J) (WT SOD1) were bred with background matched B6SJL wild type females. All mice were originally obtained from Jackson Laboratories, (Bar Harbor, ME) and bred and maintained in our in-house facility. The total DNA was isolated from tail clips of the progeny by proteinase K digestion and subsequent phenol-chloroform extraction. The progeny were genotyped using primers specific to exon 4 of the human SOD1 gene within the transgenic construct and segregated and used for subsequent studies. Transgenic mice were housed in micro-isolator cages in a barrier facility and were seronegative for mouse hepatitis virus, Sendai virus and other common viral and bacterial pathogens. The mice were observed twice a week during the first 90 days of age and subsequently monitored everyday for general health and signs of illness. Body weight was taken once a week and every day after the onset of disease. Our hSOD1G93A mice develop weakness in one or more limbs from 12 weeks of age, and reach end-stage disease 7–9 weeks after onset of limb weakness (Kim *et al.*, 2006a). CB1 knockout mice were provided by Dr. Andreas Zimmer (University of Bonn) (Zimmer *et al.*, 1999) and CB2 knockout mice were provided by Dr. George Kunos (NIH) (Jarai *et al.*, 1999). Both strains were maintained in our colony in micro-isolator cages as described above.

Spinal cord section preparation and immunohistochemistry

G93A-SOD1 transgenic mice (B6SJL-TgN[SOD1-G93A]1Gur)(G93A) and their control wild type (WT) litter mates were anesthetized and perfused with 4% PFA at several time points (5 pairs of mice for each time point). In some experiments, mice over-expressing WT SOD1 (B6SJL-TgN(SOD1)2Gur) were examined. Lumbar spinal cords were post-fixed in 4% PFA, cryoprotected in 30% sucrose and cross sectioned at 35μm thickness with a witwith microtome (SM2000R, LEICA, Bannockburn, IL USA) mated with a specimen rapid freezing unit (FRIGOMOBIL O, LEICA, Bannockburn, IL USA). Sections were

permeabilized with 0.2% TX-100, blocked by 3% BSA and 2% goat serum in PBS for overnight at 4°C. 1° and 2° antibodies were applied sequentially; each step incubated at least 20 hours at 4°C. Antibodies used: Polyclonal GluR1 (Calbiochem, San Diego, CA, USA), 1:25; Monoclonal GluR2 (BD Pharmingen, San Jose, CA, USA), 1:250; Polyclonal CB1 (Sigma-Aldrich, St. Louis, MO, USA), 1:1000; Polyclonal CB2 (Abcam, Cambridge, MA, USA), 1:500; Polyclonal CB2 (Alpha Diagnostic Intl., San Antonio, TX, USA), 1:1000; Monoclonal Synaptophysin (Sigma-Aldrich, St. Louis, MO, USA), 1:1000; Polyclonal Synaptophysin (Chemicon, Temecula, CA, USA), 1:300; Goat a mouse – FITC (Jackson ImmunoResearch Laboratories, West Grove, PA, USA), 1:100; Goat a rabbit –Cy3 (Jackson ImmunoResearch Laboratories, West Grove, PA, USA), 1:200.

Confocal microscopy and image analysis

Images were captured with a Nikon TE2000-U-based microscope system with a Nikon C1 confocal (Nikon, Melville, NY, USA). Each color channel was taken separately and averaged by 3 Kalman scans. Images were quantitatively analyzed for fluorescent intensity or colocalization by MetaMorph software (version 7.0r3) (Molecular Devices, Downingtown, PA, USA). This method has successfully been used to quantify colocalization of receptors with other markers as well as comparatively measure expression levels and colocalization in hippocampal and cortical neurons in culture (Beattie *et al.*, 2002; Leonoudakis *et al.*, 2004; Stellwagen *et al.*, 2005). This quantitative immunofluorescence method is now being extended successfully to examine receptor localization and expression in spinal cord motor neurons in tissue sections (Ferguson *et al.*, 2006). 10–20 sections from each mouse were imaged for each antibody staining combination. Five pairs of mice (G93A and control littermates) were used for each time point; 37–57 neurons from each group of mice were analyzed for each antibody. Motor neurons in the ventral horn were selected based upon the classical positional and morphological parameters used to identify motor neurons in the ventral horn of the lumbar spinal cord (Hermann *et al.*, 2001; Sun *et al.*, 2006). The neurons in each section showing a clear nucleus and a cell body diameter of 20–45μm were used for quantification.

We used average fluorescent signal intensity analysis of receptor staining on a per-soma basis to measure total expression levels (Fig 1). The "ring" of synaptophysin puncta staining surrounding the motor neuron cell body (Fig. 1B) was used as a marker to define the external limits of the somatic plasma membrane. Within the confines of this demarcation we measured the average fluorescent signal to sample receptor expression level per neuron. Sampling the protein expression level of receptors in the easily definable ventral horn motor neuron soma provides an estimate of the total neuron's receptor expression that can be used to compare SOD1 and WT expression levels. This method is similar to methods used successfully by other investigators to estimate receptor expression of motor neurons (Ferguson *et al.*, 2006). Synaptic-plasma membrane localization of GluR1, GluR2 and CB1 (which represents a subset of total surface localization) was measured by the percentage of overlapping area with synaptophysin within the whole image field (Fig. 2A). In brief, the red signal channel and the green signal channel of images were "thresholded" separately to show the red and green puncta. The term thresholding refers to the process of selecting an area of the image which has a fluorescent signal intensity that is significantly above the

average background intensity. This selection of a threshold intensity is held constant during the comparison and measurement of all experimental and control images within an experiment. The percentage of the red puncta area which overlapped with the green puncta area was calculated using Metamorph co-localization function. Since AMPARs and synaptophysin reside on separate sides of the narrow synaptic cleft, these proteins are not precisely co-localized in space. Regardless, this technique has been used successfully to detect their very close apposition (Beattie et al., 2002; Lissin et al., 1998; Stellwagen et al., 2005;(Ferguson *et al.*, 2006). To highlight co-localization of receptor and synaptophysin for presentation we utilized the Metamorph Analysis application program to display insets from the original panels (Fig. 2A). These inset panels show only areas of co-localization in white against a black background.

Data from each wild type mouse's images were grouped, averaged, and normalized to 100%. For the comparison of a G93A mouse to its WT littermate pair, data from G93A images were recalculated as relative to the mean of WT and then an average value for this mouse was calculated. Statistical significance between G93A and WT was calculated by unpaired t test. Differences were taken to be statistically significant when P<0.05.

Gene Expression Analysis

RNA extraction and gene expression analysis was performed according to published protocols (Chen *et al.*, 2004; Ignacio *et al.*, 2005). Briefly, whole spinal cords were homogenized using RNAeasy (Qiagen,Valencia, CA,USA). RNA samples were treated with RNase-free DNase to remove any genomic DNA contamination and reverse transcribed. 50 ng of cDNA from each sample used for PCR amplification with specific oligonucleotide primers using the Applied Biosystems 5700 Sequence Detection System (PE Applied Biosystems, Foster City, CA, USA). Specific primers for each gene were designed using the Primer Express Software (PE Applied Biosystems, Foster City, CA, USA). Primer lengths were 21–27 nucleotides, with a theoretical Tm of 58–60 °C. The amplicon size ranges from 66–150 bp. The specificity of the primers was demonstrated by the appearance of a single product on a 10% polyacrylamide gel and a single dissociation curve for the PCR product. All the cDNA samples were tested for genomic DNA contamination by using primers for β-actin genomic DNA; only those without genomic DNA contamination were used. In addition, the primer pairs for GluR1 and GluR2 were constructed across introns. For quantification of gene expression, the fluorescence of the SYBR Green dye bound to the PCR products was measured after each cycle and the cycle numbers recorded when the accumulated signals cross an arbitrary threshold value (C_T value). In order to normalize this value, a C_T value is determined as the difference between the C_T value for each gene and the C_T value for β-actin, which is determined in each experiment and does not vary significantly under different experimental conditions. Data from G93A were calculated as relative to WT and values from WT were normalized to 100%. Statistical significance between G93A and WT was calculated by unpaired t test. Differences were taken to be statistically significant when P<0.05.

Results

Presymptomatic changes in AMPA and cannabinoid receptors in G93A mice

Previous studies have shown that total AMPA receptor expression levels are altered during disease progression in G93A mice (Tortarolo *et al.*, 2006), however plasma membrane or synaptic localization has not been examined. In this study we measured the total expression levels and synaptic localization of AMPARs in presymptomatic G93A mice (6 weeks old). We observed staining for GluR1 and GluR2 subunits of AMPARs located both in the cell bodies and dendrites of motor neurons in ventral horn (Fig. 2A). Co-staining for AMPARs and the presynaptic marker synaptophysin allowed for the measurement of synaptic AMPARs (Fig. 2A). The receptor puncta closely apposed enough to appear overlapping (yellow) with synaptophysin puncta were classified as synaptic receptors. Images of receptor and synaptophysin staining were processed to highlight the regions of co-localization by displaying these areas in white on a black background (Co-localization inset panels, Fig. 2A). At this stage (6 weeks old) synaptic GluR1 increased significantly in G93A motor neurons (128.2 ± 10.8, $p < 0.05$) compared with WT control (100 ± 6.9) (Fig 2). In contrast, synaptic GluR2 (80.2 ± 5.0, $p < 0.01$) decreased at this stage (WT, 100 ± 6.7). Total GluR1 (96.9 ± 4.5, $p > 0.05$) did not change at 6 weeks (WT, 100 ± 5.4), while total GluR2 (86.6 ± 3.7, $p < 0.01$) decreased (WT, 100 ± 3.1).

To confirm that these changes in total expression and synaptic localization were due to the mutant properties of G93A SOD1 and not the transgene's over-expression we examined spinal cord sections from mice over-expressing WT SOD1. No significant changes in GluR1 or GluR2 total expression or synaptic localization were found in these mice (total GluR1: WT, 100 ± 5.7; WTSOD1, 108.8 ± 6.5. synaptic GluR1: WT, 100 ± 6.7; WTSOD1, 102.9 ± 8.1. total GluR2: WT, 100 ± 3.1; WTSOD1, 101 ± 3.8. synaptic GluR2: WT, 100 ± 5.3; WTSOD1, 103.7 ± 9.3) (n = 28–42 neurons analyzed from WT and WTSOD1 mice, $p > 0.05$).

Since CB1 expression in mouse spinal cord motor neurons has not been documented, we tested the specificity of our CB1 antibodies. CB1 immunostaining was present in WT mouse spinal cord sections, but not in CB1 knockout sections (Fig 3). We did not detect specific immunostaining for CB2 in motor neurons using two separate CB2 antibodies (see methods) and CB2 knockout mice as controls (data not shown). Total CB1 (WT 100 ± 8.5, G93A 84.5 ± 3.1, $p < 0.01$) decreased at 6 weeks (Fig 2B). Confocal imaging of G93A and WT sections showed that synaptic CB1 receptor expression was not altered at this stage (WT 100 ± 11.1, G93A 107.3 ± 10.5, $p > 0.05$) (Fig 2B).

Time course of changes in receptor expression during disease progression

The total expression levels of GluR1, GluR2 and CB1 were compared at several critical time points of the G93A mouse life span. We analyzed spinal cord sections from animals at 6, 10, 12 and 17 weeks of age, corresponding to presymptomatic (6 weeks), early symptomatic (10 weeks), symptomatic (12 weeks), and late stage disease (17 weeks). We restricted this analysis to the examination of total receptor expression, because synaptophysin levels decrease during disease progression in G93A mice beyond six weeks of age (Zang *et al.*,

2005). We observed a dynamic regulation of GluR1, GluR2, and CB1 expression during disease progression (Figure 4).

At 17 weeks the total GluR1 level in motor neurons increased significantly (WT 100±9.8, G93A 120.3±6.5; P<0.05)(Fig 4A). Total GluR2 levels decreased at 6 weeks (WT 100±3.1, G93A 86.6±3.7; P<0.01), were significantly higher at 12 weeks (WT 100±12.1, G93A 124.9±5.0; P<0.01), and then significantly lower at 17 weeks (WT 100±1.7, G93A 92.6±0.5; P<0.001) (Fig 4B). Total CB1 was lower at 6 weeks (WT 100±8.5, G93A 84.5±3.1; P<0.01), significantly higher at 10 weeks(WT 100±4.0, G93A 128.5±5.7; P<0.001), and lower at 17 weeks (WT 100±4.2, G93A 85.2±5.1; P<0.05) (Fig 4C). At later disease stages, it is important to note that the data represent measurements of the remaining motor neurons whose total numbers are less than in wild type littermates.

Dynamic expression of receptor genes in G93A mice

Experiments examining gene expression changes for CB1, GluR1 and GluR2 during disease progression in hSOD1G93A mice indicate that the mRNA levels of CB1 increase at 9 weeks of age (WT 100±2.8, G93A 119.0±6.3; P<0.05), followed by a decrease at 12 (WT 100±5.6, G93A 89.3±1.2; P<0.05), 15 (WT 100±3.3, G93A 88.2±1.6; P<0.01) and 18 weeks (WT 100±2.7, G93A 87.5±2.0; P<0.01) (Fig 5). Levels of GluR1 mRNA were significantly decreased at 18 weeks (end-stage) (WT 100±3.0, G93A 86.3±2.2; P<0.001). Levels of GluR2 mRNA were significantly elevated at 6 weeks (WT 100±2.7, G93A 112.7±3.5; P<0.05), followed by a trend towards declining expression that reached significance at 18 weeks (WT 100±5.0, G93A 87.7±2.4; P<0.05). For CB1, the gene expression changes preceded the protein changes.

Discussion

Recent studies have underscored the significance of both the AMPARs and the endocannabinoid system in motor neuron disease. In a study of Japanese ALS patients, impaired editing of GluR2 was observed in 56% of ALS patient motor neurons whereas GluR2 was edited in 100% of the control motor neurons (Kawahara *et al.*, 2003). In addition, an animal model of motor neuron disease can be created by increasing the number of calcium-permeable AMPARs through elevated mutant GluR2 expression in transgenic mice (Kuner *et al.*, 2005). Conversely, crossbreeding hSOD1G93A mice with transgenic mice expressing AMPARs with reduced calcium permeability results in a delay of disease onset and mortality (Tateno *et al.*, 2004). Tortarolo et al. found decreased levels of GluR2 along with increased GluR3 in motor neurons of presymptomatic hSOD1G93A mice (at 8 weeks of age), implying increased propensity to excitotoxicity (Tortarolo *et al.*, 2006). They also found that treatment of hSOD1G93A mice with ZK 187638, a non-competitive AMPAR antagonist, protected motor neurons, improved motor function and prolonged survival by >10% (Tortarolo *et al.*, 2006). Furthermore, slow and selective motor neuron death can be produced by intrathecal infusion of kainic acid; this is accompanied by increased GluR3 in affected neurons (Sun *et al.*, 2006).

The present study demonstrates for the first time that synaptic GluR1 levels are elevated prior to disease onset in the hSOD1G93A mouse model of ALS. This elevation is relevant to

disease progression since an increase in the synaptic localization and/or any change in the channel properties of AMPARs changes the excitatory profile of a neuron to a given amount of glutamate. In particular, the selective elevation of GluR1 (with no change in GluR2) suggests the presence of homomeric GluR1 AMPAR, which are calcium permeable (Leonoudakis *et al.*, 2004; Ogoshi *et al.*, 2005; Stellwagen *et al.*, 2005; Corona & Tapia, 2007). We found that synaptic GluR1 levels are increased while synaptic and total GluR2 levels are decreased in spinal cord motor neurons as early as 6 weeks of age in the G93A mouse model of ALS. To our knowledge, this is the first report of presymptomatic changes in trafficking of receptors that are in direct control of excitotoxicity and death in a mouse model of ALS.

These findings are in agreement with a recently published study demonstrating increased GluR1 mRNA and protein levels in the hippocampus in presymptomatic hSOD1G93A mice (Spalloni *et al.*, 2006). That study examined total GluR1 and GluR2 levels using Western analyses; GluR1 levels increased in hippocampus, while GluR2 levels were unchanged. The authors also performed extracellular recordings from hippocampal slices and found an increased induction and maintenance of long-term potentiation (LTP) at Schaffer collateral-CA1 synapses. This enhancement of LTP is consistent with increased plasma membrane delivery of AMPARs. The study also found superior spatial activity in mutant mice, indicative of increased cognitive ability. These data suggest that before leading to extensive neuronal excitotoxicity, the increased glutamatergic signaling in the brains of pre-symptomatic hSOD1G93A mice could mediate site-specific molecular and synaptic changes providing favorable conditions to spatial information processing. The authors conclude that the identification of pre-symptomatic behavioral changes in mouse models of ALS may point to early neural abnormalities selectively associated with mutations in the Cu/Zn superoxide dismutase (SOD1) gene.

The increase in GluR1 synaptic localization seen at 6 weeks of age may be due to increased levels of TNFα, found in the spinal cord of presymptomatic hSOD1G93A mice (Chen *et al.*, 2004; Weydt *et al.*, 2004). The proinflammatory cytokine TNFα increases cell surface and synaptic AMPARs in hippocampal neurons (Beattie *et al.*, 2002; Stellwagen *et al.*, 2005), leading to increased excitoxicity (Hermann *et al.*, 2001; Bernardino *et al.*, 2005). It is very possible that a similar situation occurs in spinal cord motor neurons during disease progression in ALS.

Recent studies have described the involvement of the endocannabinoid system in the progression of disease in hSOD1G93A mice and the benefits associated with the administration of cannabinoid agonists (Bilsland *et al.*, 2004; Raman *et al.*, 2004; Witting *et al.*, 2004; Weydt *et al.*, 2005; Kim *et al.*, 2006a; Shoemaker *et al.*, 2006). These results suggest that cannabinoid receptor-mediated processes may slow disease progression in amyotrophic lateral sclerosis and other chronic neurodegenerative diseases; (Centonze *et al.*, 2007). We found that total CB1 receptor expression was decreased at 6 weeks (presymptomatic stage), the time when synaptic GluR1 levels were elevated. At 10 weeks (symptomatic stage), CB1 levels were elevated in surviving motor neurons. This may indicate that the surviving motor neurons had enhanced levels of this "neuroprotective"

receptor. By end-stage CB1 levels are less than in controls, perhaps indicating the declining health of remaining motor neurons.

The CB2 receptor is primarily found in cells of immune origin, including microglia (Benito *et al.*, 2003; Walter *et al.*, 2003; Weydt & Moller, 2005), although neuronal expression has recently been reported (Van Sickle *et al.*, 2005; Gong *et al.*, 2006). CB2 immunostaining is increased in activated microglia from spinal cord of ALS patients (Yiangou *et al.*, 2006), and in dorsal horn neurons during inflammatory nerve damage (Wotherspoon *et al.*, 2005). We did not detect specific CB2 receptor immunostaining in spinal cord motor neurons from WT and hSOD1G93A mice using different CB2 antibodies and CB2 knockout mice as controls.

We observed dynamic regulation of AMPAR and CB1 expression during our time course analyses of immunocytochemical and gene expression changes. GluR1 protein levels appeared to increase during disease progression, reaching significance at end-stage in surviving motor neurons. This significant increase in GluR1 levels at end-stage disease may also be reflective of the insults present in the remaining motor neurons. In contrast, mRNA levels for GluR1 from whole spinal cord extracts were significantly decreased at end-stage, suggesting the increase of GluR1 protein in motor neurons could not compensate the motor neuron loss and GluR1 may decrease in astrocytes or in other neurons in the spinal cord late in the disease process in G93A mice. For CB1, the alteration in gene expression preceded the protein changes.

GluR2 levels in motor neurons were tightly regulated. As discussed above, at the presymptomatic stage (6 weeks), these were decreased. This result is in agreement with those of Tortarolo et al, who found decreased levels of GluR2 in motor neurons of presymptomatic hSOD1G93A mice (at 8 weeks of age)(Tortarolo *et al.*, 2006). In contrast, at 6 weeks we found a $12.7 \pm 3.5\%$ increase in mRNA levels as compared to WT controls. Tortarolo et al (2006) also observed a trend towards increased GluR2 mRNA in motor neurons at 8 weeks in the G93A mice. Together, these studies suggest that post-transcriptional mechanisms may be involved in the GluR2 downregulation. Interestingly, as GluR2 mRNA editing is also post-transcriptional (Pellegrini-Giampietro *et al.*, 1997; Kawahara *et al.*, 2003), post-transcriptional defects could relate to both changes in both amount and editing state of the protein. We found increases in synaptic GluR1 levels, whereas Tortarolo and colleagues (2006) found increased total GluR3 levels at this stage of the disease; however, both studies indicated increased propensity to excitotoxicity due to altered composition of AMPARs. At 12 weeks, GluR2 levels were significantly increased. As the disease progressed further, GluR2 levels decreased in the remaining motor neurons, with a significant decrease relative to controls at end-stage. It is possible, that as with CB1, the surviving motor neurons expressed more GluR2 as a defense mechanism, which was ultimately overwhelmed at end-stage disease. Alternatively, these changes may be compensatory in response to the decreased number of motor neurons. That is, at end-stage of the disease the remaining motor neurons may need a higher number of GluR1, lower number of Glu2 and lower CB1 to increase their excitability in order to compensate for the decreased number of motor neurons.

In summary, we have used quantitative immunofluorescent analysis of spinal cord motor neurons to survey total protein expression and synaptic localization of two subtypes of the excitatory AMPARs and the inhibitory CB1 cannabinoid receptor in the G93A mouse model of ALS. We have found significant differences between G93A and WT mice at an important early time point that precedes the first appearance of ALS-like symptoms. At this early time point, our data showing that GluR1 AMPAR subunits are increased at synapses while synaptic *and* total GluR2 AMPAR subunits are decreased is consistent with a greater-than-normal synaptic localization of GluR1 homomeric AMPARs. In concert with these changes we find that total expression levels of the CB1 cannabinoid receptor (which is protective against excitotoxicity) are reduced at this early time point. We propose that early increases in the amounts of inflammatory cytokines (eg- TNFα) leads to these trafficking and expression changes in these important excitatory and inhibitory receptor classes that together determine a motor neuron's vulnerability to glutamatergic excitotoxicity. Our current studies aimed at confirming this hypothesis and detailing the underlying signaling mechanisms that are responsible for these changes have the potential to uncover a new set of drug targets to be used in the fight against ALS.

Acknowledgments

Abbreviations

ALS	amyotrophic lateral sclerosis
AMPARs	α-amino-3-hydroxy-5-methyl-4-isoxazolepropionic acid receptors
CB1	cannabinoid receptor 1
GluR1	glutamate receptor 1
GluR2	glutamate receptor 2
hSOD1	human Cu/Zn superoxide dismutase 1
LTP	long-term potentiation
^{9}-THC	^{9}-tetrahydrocannabinol
TNFα	Tumor necrosis factor α
WT	wild type

References

Abood ME, Rizvi G, Sallapudi N, McAllister SD. Activation of the CB(1) cannabinoid receptor protects cultured mouse spinal neurons against excitotoxicity. Neurosci Lett. 2001; 309:197–201. [PubMed: 11514075]

Bar-Peled O, O'Brien RJ, Morrison JH, Rothstein JD. Cultured motor neurons possess calcium-permeable AMPA/kainate receptors. Neuroreport. 1999; 10:855–859. [PubMed: 10208560]

Beattie EC, Stellwagen D, Morishita W, Bresnahan JC, Ha BK, Von Zastrow M, Beattie MS, Malenka RC. Control of synaptic strength by glial TNFalpha. Science. 2002; 295:2282–2285. [PubMed: 11910117]

Benito C, Nunez E, Tolon RM, Carrier EJ, Rabano A, Hillard CJ, Romero J. Cannabinoid CB2 receptors and fatty acid amide hydrolase are selectively overexpressed in neuritic plaque-associated glia in Alzheimer's disease brains. J Neurosci. 2003; 23:11136–11141. [PubMed: 14657172]

Bernardino L, Xapelli S, Silva AP, Jakobsen B, Poulsen FR, Oliveira CR, Vezzani A, Malva JO, Zimmer J. Modulator effects of interleukin-1beta and tumor necrosis factor-alpha on AMPA-induced excitotoxicity in mouse organotypic hippocampal slice cultures. J Neurosci. 2005; 25:6734–6744. [PubMed: 16033883]

Bilsland L, Pryce G, Baker D, Greensmith L. The Neuroprotective effects of cannabinoids in the SOD1G93A mouse model of ALS. Amyotrophic Later Scler & Motor Neuron Disord. 2004; 5:92.

Boillee S, Vande Velde C, Cleveland DW. ALS: A Disease of Motor Neurons and Their Nonneuronal Neighbors. Neuron. 2006; 52:39–59. [PubMed: 17015226]

Brown RH Jr. Amyotrophic lateral sclerosis. Insights from genetics. Arch Neurol. 1997; 54:1246–1250. [PubMed: 9341570]

Carriedo S, Yin H, Weiss J. Motor neurons are selectively vulnerable to AMPA/kainate receptor-mediated injury in vitro. J Neurosci. 1996; 16:4069–4079. [PubMed: 8753869]

Centonze D, Rossi S, Finazzi-Agro A, Bernardi G, Maccarrone M. The (endo)cannabinoid system in multiple sclerosis and amyotrophic lateral sclerosis. Int Rev Neurobiol. 2007; 82:171–186. [PubMed: 17678961]

Chen L-C, Smith Ap, Yong B, Zukic B, Ignacio S, Moore DH, M LN. Temporal gene expression patterns in G93A/SOD1 mouse. Amyotroph Lateral Scler Other Motor Neuron Disord. 2004; 5:164–171. [PubMed: 15512905]

Cleveland DW, Rothstein JD. From Charcot to Lou Gehrig: deciphering selective motor neuron death in ALS. Nat Rev Neurosci. 2001; 2:806–819. [PubMed: 11715057]

Corona JC, Tapia R. Ca(2+)-permeable AMPA receptors and intracellular Ca(2+) determine motoneuron vulnerability in rat spinal cord in vivo. Neuropharmacology. 2007

Ferguson AR, Christensen RN, Gensel JC, Miller BA, Beattie EC, Bresnahan JC, Beattie MS. Effect of Tumor Necrosis Factor-Alpha on AMPA-type glutamate receptor trafficking in spinal cord neurons in vivo. Proceedings of the 2006 Abstract Viewer and Itinerary Planner, Society for Neuroscience. :475.411. (Year) City.

Gong JP, Onaivi ES, Ishiguro H, Liu QR, Tagliaferro PA, Brusco A, Uhl GR. Cannabinoid CB2 receptors: immunohistochemical localization in rat brain. Brain Res. 2006; 1071:10–23. [PubMed: 16472786]

Gurney ME, Cutting FB, Zhai P, Doble A, Taylor CP, Andrus PK, Hall ED. Benefit of vitamin E, riluzole, and gabapentin in a transgenic model of familial amyotrophic lateral sclerosis. Ann Neurol. 1996; 39:147–157. [PubMed: 8967745]

Hermann GE, Rogers RC, Bresnahan JC, Beattie MS. Tumor necrosis factor-alpha induces cFOS and strongly potentiates glutamate-mediated cell death in the rat spinal cord. Neurobiol Dis. 2001; 8:590–599. [PubMed: 11493024]

Ignacio S, Moore DH, Smith AP, Lee NM. Effect of neuroprotective drugs on gene expression in G93A/SOD1 mice. Ann N Y Acad Sci. 2005; 1053:121–136. [PubMed: 16179515]

Jarai Z, Wagner J, Varga K, Lake K, Compton D, Martin B, Zimmer A, Bonner T, Buckley N, Mezey E, Razdan R, Zimmer A, Kunos G. Cannabinoid-induced mesenteric vasodilation through an endothelial site distinct from CB1 or CB2 receptors. Proc Natl Acad Sci U S A. 1999; 96:14136–14141. [PubMed: 10570211]

Kawahara Y, Kwak S, Sun H, Ito K, Hashida H, Aizawa H, Jeong SY, Kanazawa I. Human spinal motoneurons express low relative abundance of GluR2 mRNA: an implication for excitotoxicity in ALS. J Neurochem. 2003; 85:680–689. [PubMed: 12694394]

Kim K, Moore DH, Makriyannis A, Abood ME. AM1241, a cannabinoid CB2 receptor selective compound, delays disease progression in a mouse model of amyotrophic lateral sclerosis. Eur J Pharmacol. 2006a; 542:100–105. [PubMed: 16781706]

Kim SH, Won SJ, Mao XO, Jin K, Greenberg DA. Molecular mechanisms of cannabinoid protection from neuronal excitotoxicity. Mol Pharmacol. 2006b; 69:691–696. [PubMed: 16299067]

Klivenyi P, Ferrante RJ, Matthews RT, Bogdanov MB, Klein AM, Andreassen OA, Mueller G, Wermer M, Kaddurah-Daouk R, Beal MF. Neuroprotective effects of creatine in a transgenic animal model of amyotrophic lateral sclerosis. Nat Med. 1999; 5:347–350. [PubMed: 10086395]

Kuner R, Groom AJ, Bresink I, Kornau HC, Stefovska V, Muller G, Hartmann B, Tschauner K, Waibel S, Ludolph AC, Ikonomidou C, Seeburg PH, Turski L. Late-onset motoneuron disease caused by a functionally modified AMPA receptor subunit. Proc Natl Acad Sci U S A. 2005; 102:5826–5831. Epub 2005 Apr 5812. [PubMed: 15827116]

Leonoudakis D, Braithwaite SP, Beattie MS, Beattie EC. TNFalpha-induced AMPA-receptor trafficking in CNS neurons; relevance to excitotoxicity? Neuron Glia Biol. 2004; 1:263–273. [PubMed: 16520832]

Ludolph AC, Meyer T, Riepe MW. The role of excitotoxicity in ALS--what is the evidence? J Neurol. 2000; 247:I7-16. [PubMed: 10795882]

Ogoshi F, Yin HZ, Kuppumbatti Y, Song B, Amindari S, Weiss JH. Tumor necrosis-factor-alpha (TNF-alpha) induces rapid insertion of Ca2+-permeable alpha-amino-3-hydroxyl-5-methyl-4-isoxazole-propionate (AMPA)/kainate (Ca-A/K) channels in a subset of hippocampal pyramidal neurons. Exp Neurol. 2005; 193:384–393. [PubMed: 15869941]

Pellegrini-Giampietro DE, Gorter JA, Bennett MV, Zukin RS. The GluR2 (GluR-B) hypothesis: Ca(2+)-permeable AMPA receptors in neurological disorders. Trends Neurosci. 1997; 20:464–470. [PubMed: 9347614]

Raman C, McAllister SD, Rizvi G, Patel SG, Moore DH, Abood ME. Amyotrophic lateral sclerosis: delayed disease progression in mice by treatment with a cannabinoid. Amyotroph Lateral Scler Other Motor Neuron Disord. 2004; 5:33–39. [PubMed: 15204022]

Robberecht W. Oxidative stress in amyotrophic lateral sclerosis. J Neurol. 2000; 247:I1–I6. [PubMed: 10795881]

Rosen D, Siddique T, Patterson D, Figlewicz D, Sapp P, Hentati A, Donaldson D, Goto J, O'Regan J, Deng H, Rahmani Z, Krizus A, McKenna-Yasek D, Cayabyab A, Gaston S, Berger R, Tanzi R, Halperin J, Herzfeldt B, Bergh RVd, Hung W-Y, Bird T, Deng G, Mulder D, Smyth C, Laing N, Soriano E, Pericak-Vance M, Haines J, Rouleau G, Gusella J, Horvitz H, R B Jr. Mutations in Cu/Zn superoxide dismutase gene are associated with familial amyotrophic lateral sclerosis. Nature. 1993; 362:59–62. [PubMed: 8446170]

Roy J, Minotti S, Dong L, Figlewicz D, Durham H. Glutamate potentiates the toxicity of mutant Cu/Zn-superoxide dismutase in motor neurons by postsynaptic calcium-dependent mechanisms. J Neurosci. 1998; 18:9673–9684. [PubMed: 9822728]

Shoemaker JL, Seely KA, Reed RL, Crow JP, Prather P. The CB2 cannabinoid agonist AM-1241 prolongs survival in a transgenic mouse model of amyotrophic lateral sclerosis when initiated at symptom onset. Journal of Neurochemistry. 2006 online.

Spalloni A, Geracitano R, Berretta N, Sgobio C, Bernardi G, Mercuri NB, Longone P, Ammassari-Teule M. Molecular and synaptic changes in the hippocampus underlying superior spatial abilities in pre-symptomatic G93A+/+ mice overexpressing the human Cu/Zn superoxide dismutase (Gly93 -->ALA) mutation. Exp Neurol. 2006; 197:505–514. [PubMed: 16309674]

Stellwagen D, Beattie EC, Seo JY, Malenka RC. Differential regulation of AMPA receptor and GABA receptor trafficking by tumor necrosis factor-alpha. J Neurosci. 2005; 25:3219–3228. [PubMed: 15788779]

Sun H, Kawahara Y, Ito K, Kanazawa I, Kwak S. Slow and selective death of spinal motor neurons in vivo by intrathecal infusion of kainic acid: implications for AMPA receptor-mediated excitotoxicity in ALS. J Neurochem. 2006; 98:782–791. [PubMed: 16893420]

Tateno M, Sadakata H, Tanaka M, Itohara S, Shin RM, Miura M, Masuda M, Aosaki T, Urushitani M, Misawa H, Takahashi R. Calcium-permeable AMPA receptors promote misfolding of mutant SOD1 protein and development of amyotrophic lateral sclerosis in a transgenic mouse model. Hum Mol Genet. 2004; 13:2183–2196. Epub 2004 Aug 2184. [PubMed: 15294873]

Tortarolo M, Grignaschi G, Calvaresi N, Zennaro E, Spaltro G, Colovic M, Fracasso C, Guiso G, Elger B, Schneider H, Seilheimer B, Caccia S, Bendotti C. Glutamate AMPA receptors change in motor

neurons of SOD1G93A transgenic mice and their inhibition by a noncompetitive antagonist ameliorates the progression of amytrophic lateral sclerosis-like disease. J Neurosci Res. 2006; 83:134–146. [PubMed: 16323214]

Van Sickle MD, Duncan M, Kingsley PJ, Mouihate A, Urbani P, Mackie K, Stella N, Makriyannis A, Piomelli D, Davison JS, Marnett LJ, Di Marzo V, Pittman QJ, Patel KD, Sharkey KA. Identification and functional characterization of brainstem cannabinoid CB2 receptors. Science. 2005; 310:329–332. [PubMed: 16224028]

Vandenberghe W, Robberecht W, Brorson J. AMPA receptor calcium permeability, GluR2 expression, and selective motoneuron vulnerability. J Neurosci. 2000; 20:123–132. [PubMed: 10627588]

Walter L, Franklin A, Witting A, Wade C, Xie Y, Kunos G, Mackie K, Stella N. Nonpsychotropic cannabinoid receptors regulate microglial cell migration. J Neurosci. 2003; 23:1398–1405. [PubMed: 12598628]

Weydt P, Hong S, Witting A, Moller T, Stella N, Kliot M. Cannabinol delays symptom onset in SOD1 (G93A) transgenic mice without affecting survival. Amyotroph Lateral Scler Other Motor Neuron Disord. 2005; 6:182–184. [PubMed: 16183560]

Weydt P, Moller T. Neuroinflammation in the pathogenesis of amyotrophic lateral sclerosis. Neuroreport. 2005; 16:527–531. [PubMed: 15812300]

Weydt P, Yuen EC, Ransom BR, Moller T. Increased cytotoxic potential of microglia from ALS-transgenic mice. Glia. 2004; 48:179–182. [PubMed: 15378658]

Witting A, Weydt P, Hong S, Kliot M, Moller T, Stella N. Endocannabinoids accumulate in spinal cord of SOD1 G93A transgenic mice. J Neurochem. 2004; 89:1555–1557. [PubMed: 15189359]

Wotherspoon G, Fox A, McIntyre P, Colley S, Bevan S, Winter J. Peripheral nerve injury induces cannabinoid receptor 2 protein expression in rat sensory neurons. Neuroscience. 2005; 135:235–245. [PubMed: 16084654]

Yiangou Y, Facer P, Durrenberger P, Chessell IP, Naylor A, Bountra C, Banati RR, Anand P. COX-2, CB2 and P2X7-immunoreactivities are increased in activated microglial cells/macrophages of multiple sclerosis and amyotrophic lateral sclerosis spinal cord. BMC Neurol. 2006; 6:12. [PubMed: 16512913]

Zang DW, Lopes EC, Cheema SS. Loss of synaptophysin-positive boutons on lumbar motor neurons innervating the medial gastrocnemius muscle of the SOD1G93A G1H transgenic mouse model of ALS. J Neurosci Res. 2005; 79:694–699. [PubMed: 15668955]

Zhu S, Stavrovskaya IG, Drozda M, Kim BY, Ona V, Li M, Sarang S, Liu AS, Hartley DM, Wu du C, Gullans S, Ferrante RJ, Przedborski S, Kristal BS, Friedlander RM. Minocycline inhibits cytochrome c release and delays progression of amyotrophic lateral sclerosis in mice. Nature. 2002; 417:74–78. [PubMed: 11986668]

Zimmer A, Zimmer A, Hohmann A, Herkenham M, Bonner T. Increased mortality, hypoactivity, and hypoalgesia in cannabinoid CB1 receptor knockout mice. Proc Natl Acad Sci U S A. 1999:5780–5785. [PubMed: 10318961]
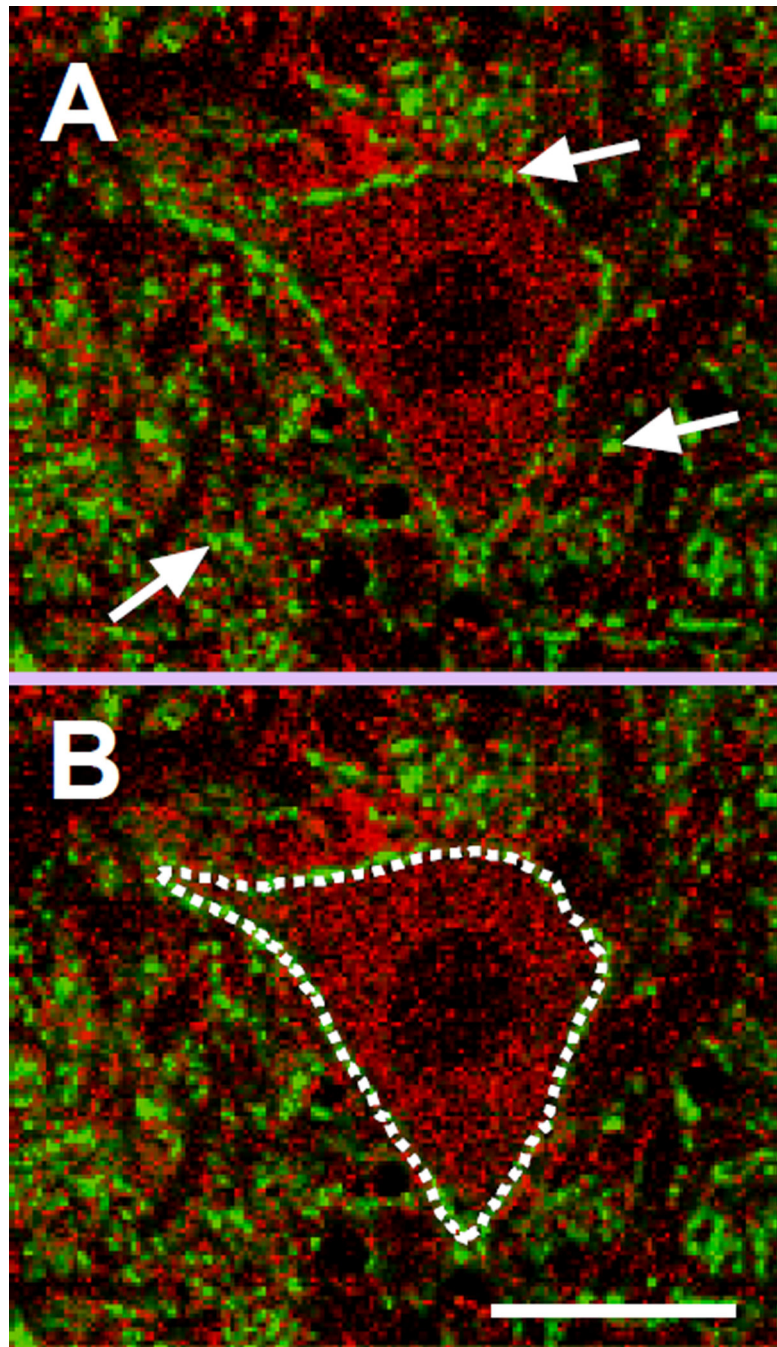
Figure 1. Confocal imaging of mouse spinal cord samples and quantification method
(A) A representative confocal image of a ventral horn spinal cord motor neuron showing GluR1 (red) and synaptophysin (green) staining. Only images of motor neurons located in the lower half of the ventral horn showing a clear nucleus and with a cell body diameter of 20–45μm were used for quantification. Synaptic localization of GluR1, GluR2, and CB1 was measured by the level of percentage of overlapping area with synaptophysin in the whole image field. The white arrows pointing to yellow puncta indicate the synaptic localization of GluR1.

(B) A "ring" of synaptophysin puncta staining surrounding the neuron soma, marked by the white dotted line, was used to define the plasma membrane. The average intensity of the fluorescent signal inside this demarcation was used to quantify total expression levels. Scale bar, 20μm.
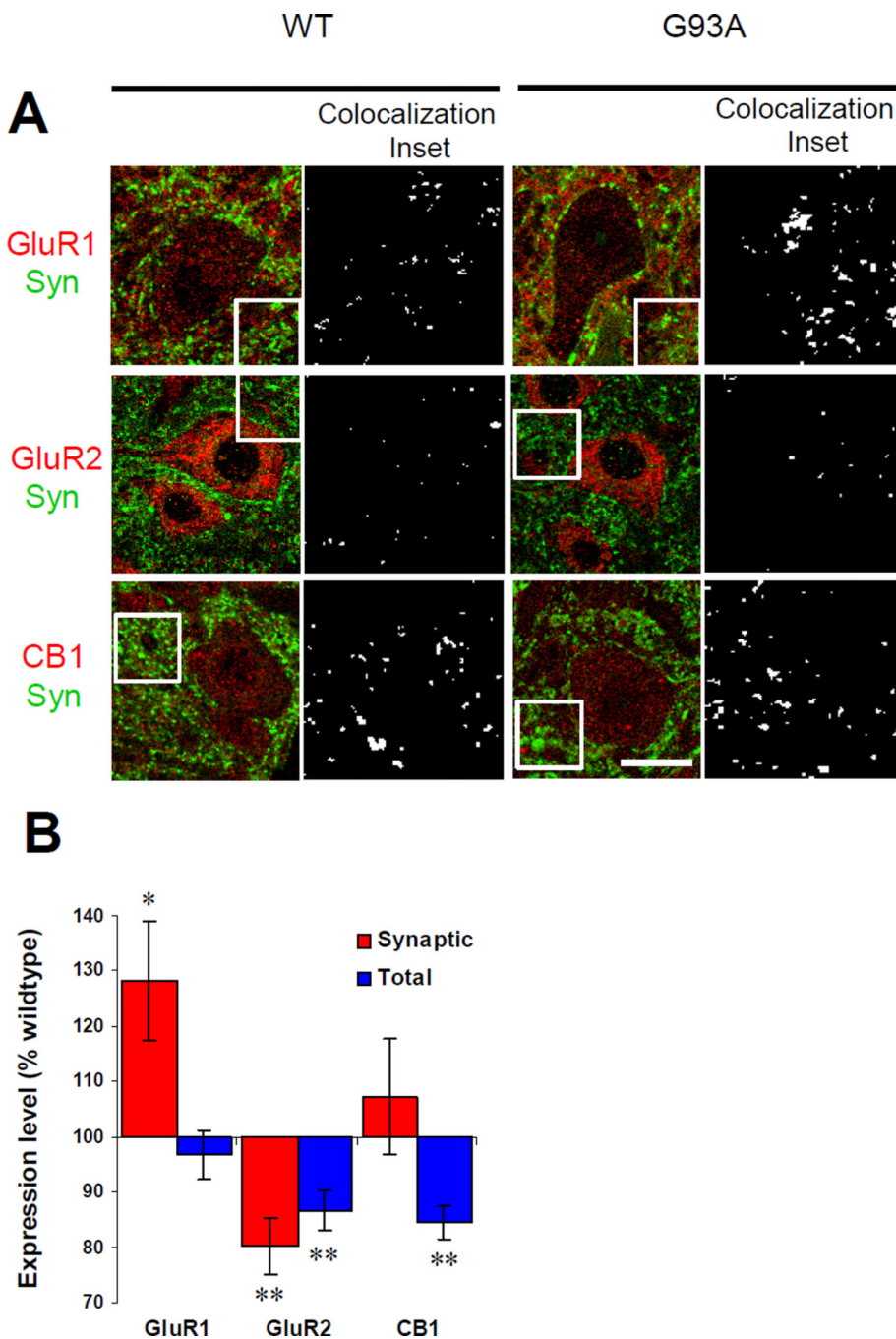
Figure 2. Presymptomatic changes of AMPA and CB1 receptors in ventral horn motor neurons of G93A mice

(A) Staining for GluR1, GluR2 and CB1 (red) and co-staining for synaptophysin (green) in sections from 6 week old wild type littermate control and G93A mice. Synaptophysin puncta outline motor neuron cell bodies. Punctate GluR1, GluR2 and CB1 staining was observed in neuronal cytoplasm as well as in somatic and dendritic plasma membrane. Receptors were defined as localized to the plasma membrane by co-localization with synaptophysin. Examples of synaptically localized receptors that are apposition or co-localization with

synaptophysin puncta are highlighted in the black and white panels to the right of the green and red panels. These black and white panels are derived from insets defined by the boxed area in the green and red panels and white marks areas of receptor and synaptophysin co-localization. Scale bars in green and red panels, 20μm. Width of black and white co-localization inset panels, 19μm.

(B) Levels of synaptic and total receptor expression in motor neurons of G93A mice. Values from G93A mice are represented as percentages of wild type values. Synaptic GluR1 increased significantly at this presymptomatic stage. Synaptic and total GluR2 both decreased significantly. Total CB1 receptor decreased significantly. *P<0.05, **P<0.01. Error bars represent SEM. Sample number (N= 37–57 neurons analyzed from G93A and control mice):
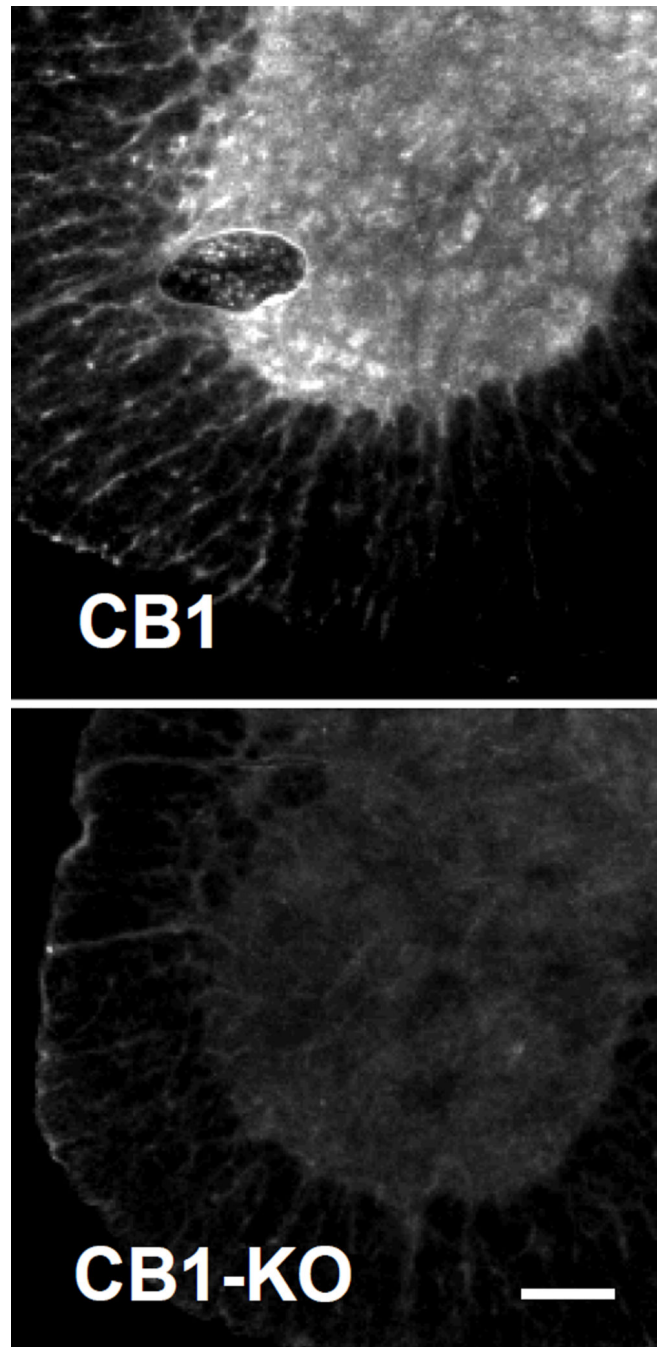
Figure 3. CB1 Cannabinoid receptor is present in motor neurons
Spinal cord sections from a wild type mouse (top panel) and a CB1 KO mouse (bottom panel) were stained with CB1 antibody. Representative ventral horns images are shown. CB1 antibody staining showed positive bright puncta in motor neurons in the wild type mouse spinal cord section, while only weak background staining was observed in the CB1 KO section. Scale bar, 100μm.
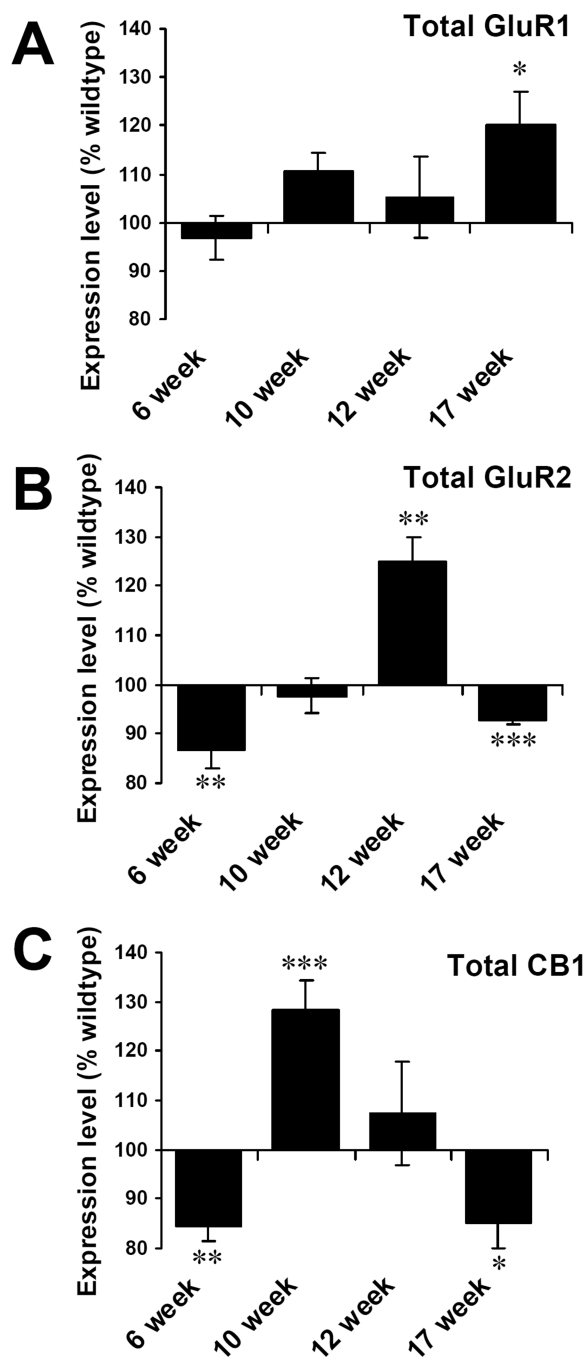
Figure 4. Time course changes of total receptor changes in G93A mice

Levels of total expression in motor neurons of G93A mice are represented as percentages of wild type littermate controls of the same time points. **(A)** Total GluR1 increased significantly at 17 weeks. **(B)** Total GluR2 decreased at 6 weeks, then increased at 12 weeks. Finally total GluR2 decreased again at 17 weeks. **(C)** Total CB1 decreased early (6 weeks), increased at 10 weeks, and decreased at 17 weeks. Unpaired t test. *P<0.05, **P<0.01, ***P<0.001. Error bars represent SEM. N = 37–57 neurons analyzed from G93A and control mice for each time point.
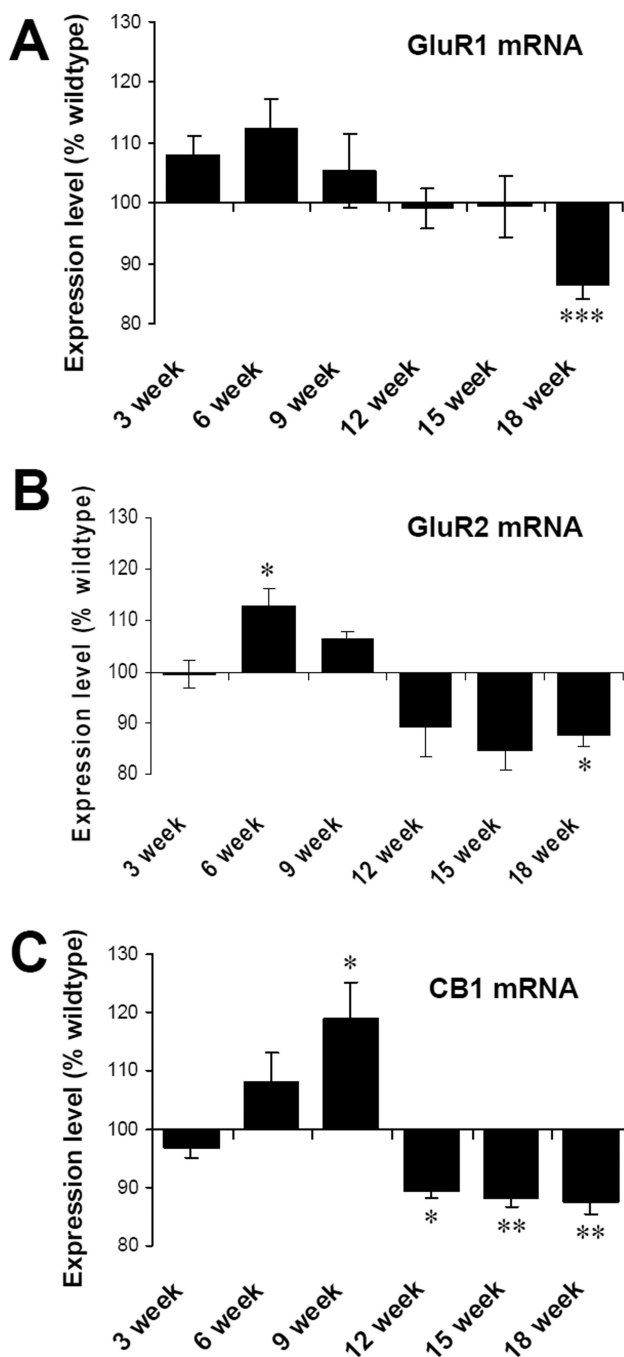
Figure 5. Dynamic regulation of gene expression changes in hSOD1G93A mice
Levels of mRNA in G93A spinal cords are represented as percentages of wildtype controls of the same time points. (**A**) GluR1 mRNA in G93A spinal cords showed a significant decrease at 18 week. (**B**) GluR2 mRNA increased at 6 weeks and decreased at 18 weeks. (**C**) CB1 mRNA increased significantly at 9 week, while decreased at 12, 15 and 18 week. N = 10 spinal cord preparations in each group. Unpaired t test. * p<0.05; ** p<0.01, ***p<0.001. Error bars represent SEM.